JACS
JOURNAL OF THE AMERICAN CHEMICAL SOCIETY
Article
pubs.acs.org/JACS

Concepts for Stereoselective Acrylate Insertion

Boris Neuwald,[†] Lucia Caporaso,*[,‡] Luigi Cavallo,[§] and Stefan Mecking*[,†]

[†]Chair of Chemical Materials Science, Department of Chemistry, University of Konstanz, 78464 Konstanz, Germany
[‡]Department of Chemistry and Biology, University of Salerno, Via Ponte Don Melillo, 84084-Fisciano (SA), Italy
[§]Physical Sciences and Engineering, Kaust Catalysis Center, King Abdullah University of Science and Technology (KAUST), Thuwal 23955-6900, Saudi Arabia

Supporting Information

ABSTRACT: Various phosphinesulfonato ligands and the corresponding palladium complexes [{((P^O)PdMeCl)-μ-M}$_n$] ([{(^{X}**1-Cl**)-μ-M}$_n$], (P^O) = κ^2-*P*,*O*-Ar$_2$*P*C$_6$H$_4$SO$_2$*O*) with symmetric (Ar = 2-MeOC$_6$H$_4$, 2-CF$_3$C$_6$H$_4$, 2,6-(MeO)$_2$C$_6$H$_3$, 2,6-(*i*PrO)$_2$C$_6$H$_3$, 2-(2′,6′-(MeO)$_2$C$_6$H$_3$)C$_6$H$_4$) and asymmetric substituted phosphorus atoms (Ar^1 = 2,6-(MeO)$_2$C$_6$H$_3$, Ar^2 = 2′-(2,6-(MeO)$_2$C$_6$H$_3$)C$_6$H$_4$; Ar^1 = 2,6-(MeO)$_2$C$_6$H$_3$, Ar^2 = 2-*c*HexOC$_6$H$_4$) were synthesized. Analyses of molecular motions and dynamics by variable temperature NMR studies and line shape analysis were performed for the free ligands and the complexes. The highest barriers of $\Delta G^{\ddagger}$ = 44−64 kJ/mol were assigned to an aryl rotation process, and the flexibility of the ligand framework was found to be a key obstacle to a more effective stereocontrol. An increase of steric bulk at the aryl substituents raises the motional barriers but diminishes insertion rates and regioselectivity. The stereoselectivity of the first and the second methyl acrylate (MA) insertion into the Pd−Me bond of in situ generated complexes ^{X}**1** was investigated by NMR and DFT methods. The substitution pattern of the ligand clearly affects the first MA insertion, resulting in a stereoselectivity of up to 6:1 for complexes with an asymmetric substituted phosphorus. In the consecutive insertion, the stereoselectivity is diminished in all cases. DFT analysis of the corresponding insertion transition states revealed that a selectivity for the first insertion with asymmetric (P^O) complexes is diminished in the consecutive insertions due to uncooperatively working enantiomorphic and chain end stereocontrol. From these observations, further concepts are developed.

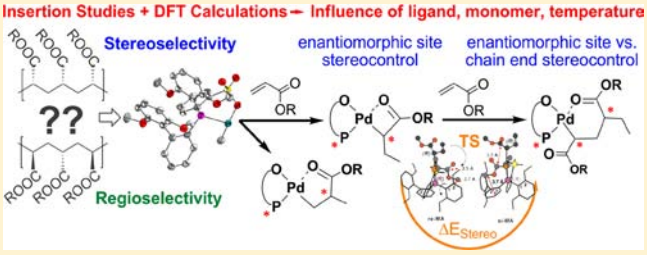

INTRODUCTION

The regularity of stereocenters in a polymeric chain can profoundly affect the macroscopic material properties. This is illustrated most impressively by isotactic polypropylene, produced on the 10^7 ton/year scale. These materials are prepared by catalytic insertion polymerization, in principle the most powerful and generic concept for stereoregular polymerization. However, stereoselective insertion polymerization is restricted to date to nonpolar olefins, and excludes polar vinyl monomers. Isotactic and syndiotactic PMMA can be prepared by a coordination−addition mechanism akin to anionic polymerization with early transition metal catalysts. However, acrylates are not amenable to these polymerizations, due to the sterically less bulky and chemically more reactive proton in α-position.[1]

Isotactic polymers can be obtained from alkyl acrylates by anionic polymerization at low temperatures,[2,3] with chiral zirconocenes by a proposed site-controlled addition mechanism,[4] or with chiral auxiliary controlled free radical polymerization.[5] Preparation of syndiotactic material proved to be even more difficult. Slightly syndioenriched (up to ∼63% r-dyads) poly(*tert*-butyl acrylate) can be obtained if the polymerization is initiated by *t*BuLi in the presence of organoaluminium complexes,[6] or by free radical polymerization at low temperatures.[7]

Conclusively so far not only a broad and universal way of influencing the stereocontrol of alkyl acrylate polymerization is missing, but there is also a conceptual gap to an effective tunable control mechanism. Insertion polymerization is a very effective and versatile approach to control the tacticity in polypropylene homo- and copolymers as underlined by the successful industrial application of metallocene catalysts.[8,9] The clear advantage of insertion polymerization for stereocontrol is that chain growth proceeds directly at the metal center to which the growing chiral polymer chain and an (un)symmetric ligand are attached in close proximity, enabling control of the insertion mode of the next prochiral monomer via a chain end or enantiomorphic site stereocontrol mechanism.

Before this general background, stereoselective alkyl acrylate polymerization by insertion in principle appears a promising approach. However, insertion polymerization of polar-substituted vinyl monomers had remained elusive for a long time. Copolymerization of polar vinyl monomers with ethylene was achieved first with cationic Pd(II) diimine complexes. In this

Received: August 16, 2012
Published: December 20, 2012

dx.doi.org/10.1021/ja3101787 | J. Am. Chem. Soc. 2013, 135, 1026−1036

case, highly branched copolymers, which consist of ethylene as major component (≥75 mol %) and contain acrylate units at the end of the branches preferentially, were obtained.[10−12] The extensive chain walking appears problematic in advancing toward any stereoselective polymerizations. To this end, the discovery that neutral arylphosphinesulfonato Pd(II) complexes are able to copolymerize methyl acrylate (MA) and ethylene to linear random copolymers represented a major improvement.[13] The development of weakly coordinated catalyst precursors ([(P^O)PdMe(L)] with L = DMSO, also cf., Scheme 1) or

Scheme 1. Numbering of Complexes

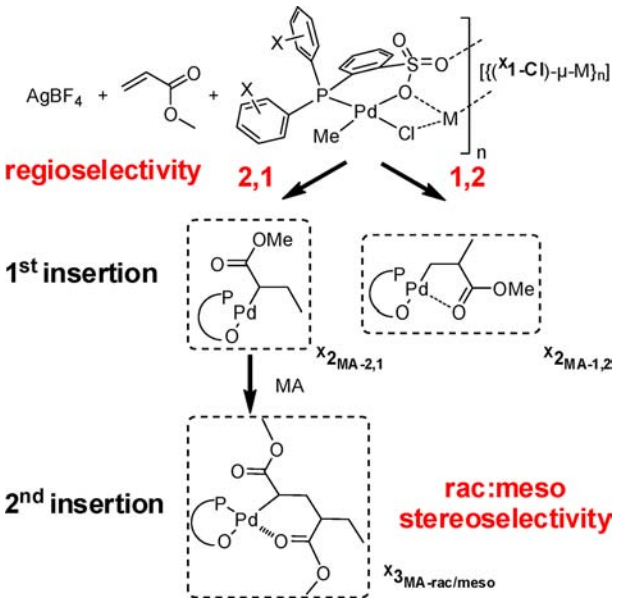

rather in situ generated complexes entirely free of an additional monodentate ligand L allowed for isolation of ethylene copolymers with polar monomer incorporation of up to 50 mol %. In addition, these weakly coordinated catalyst precursors enabled insertion homopolymerization of MA to products with degrees of oligomerization up to ca. DP_n = 5−7.[14,15] A mechanistic study of the underlying steps clearly revealed that this acrylate homopolymerization occurs by an insertion mechanism. For example, a six-membered chelate complex [(P^O)Pd{κ^2-*C*,*O*-CH(C(O)OMe)CH_2CH(C(*O*)-OMe)CH_2CH_3}] results from two consecutive MA insertions into the Pd−Me bond.[16] Interestingly, this six-membered chelate was obtained as a mixture of two diastereomers in a ca. 2:1 ratio arising from the configuration of the two stereocenters at the methyl acrylate derived methine groups.

For comparison to proven concepts of stereocontrol in olefin polymerization, early transition metal metallocene and phenoxy-imine/amine post metallocene catalysts are instructive. These catalysts all show a tetrahedral or octahedral coordination sphere around the central atom, which allows for a space filling surrounding of the active center. Typically, the multidentate ligand and the growing chain arrange and determine the preferred monomer enantioface. An illustrative exception is the C_2 symmetric unbridged phenoxy-imine catalyst, which is regarded as rather fluxional resulting in the production of a syndiotactic polymer by a chain end control mechanism.[1,8,17−20]

Stereoselective insertion polymerization with late transition metal catalysts has been less studied. In this case, the metal center is significantly less crowded than for the aforementioned early transition metal catalysts. However, the stereoselective Pd-catalyzed copolymerization of CO with vinyl monomers like propylene and styrene has been described. Achiral, symmetric diimine, or bipyridine (N^N) ligands lead to syndiotactic styrene copolymers by a chain-end stereocontrol, whereas the enantiomorphic site-controlled formation of isotactic polymer was described for C_2 and C_1 symmetric (N^N) and (P^N) ligands.[1,21−23] In addition, also the formation of highly isotactic propylene/CO copolymers has been described for bisphosphine and phosphine/phosphite ligands of various symmetries.[23−26]

For (P^O)Pd systems, the bidentate phosphine-sulfonato ligand exhibits two completely different coordination sites at the metal, and the exact combination of the hard sulfonate with the soft phosphine donor seems to be a prerequisite for the unique properties of this catalytic system.[27,28] Whereas the steric bulk of the phosphine substituents can be adjusted and will have a distinct influence on the active center, the sulfonic acid moiety is rather small and does not offer a possibility for steric variation. This results in two completely open sides around the SO_3-group, and in general a relatively high flexibility of the ligand (Figure 1). Crystallographic structures and DFT

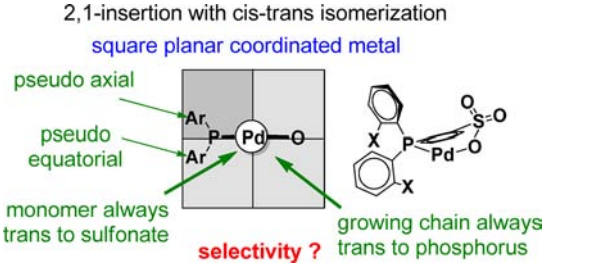

Figure 1. Analysis of square planar (P^O)Pd catalyst in regard to possible stereoselectivity. The grayer top-left quadrant, where the pseudo-axial Ar ligand is located, is sterically more crowded than the other quadrants.

studies indicate that one of the nonbackbone aryl substituents at phosphorus adopts a pseudoaxial position and is twisted toward the palladium center, while the other substituent adopts a pseudoequatorial position with a larger distance to the central atom.[16] Overall, this can be visualized in a quadrant scheme as depicted in Figure 1 where only one quadrant is accentuated as distinctly sterically crowded.

In contrast to the migratory insertion mechanism for early transition metals, monomer insertion at (P^O)Pd system only occurs after cis/trans isomerization of the growing chain and the coordinated monomer, so that insertion always occurs from the isomer in which the olefin is cis to the P-donor.[16,27] The structural features enabling this acrylate insertion mechanism are a highly unsymmetric bidentate ligand not only in terms of soft/hard donor characteristics but also in terms of the steric demand of the two donors.[29] We now report an analysis of stereocontrol mechanisms in such unsymmetrical environments.

RESULTS AND DISCUSSION

Acrylate insertions into phosphinesulfonato palladium methyl complexes (^{X}**1**) to afford the single (^{X}**2**) and double (^{X}**3**) insertion products were investigated (Scheme 1).

dx.doi.org/10.1021/ja3101787 | *J. Am. Chem. Soc.* 2013, 135, 1026−1036

A range of substitution patterns at phosphorus differing in steric bulk, flexibility, and symmetry were studied (Figure 2),

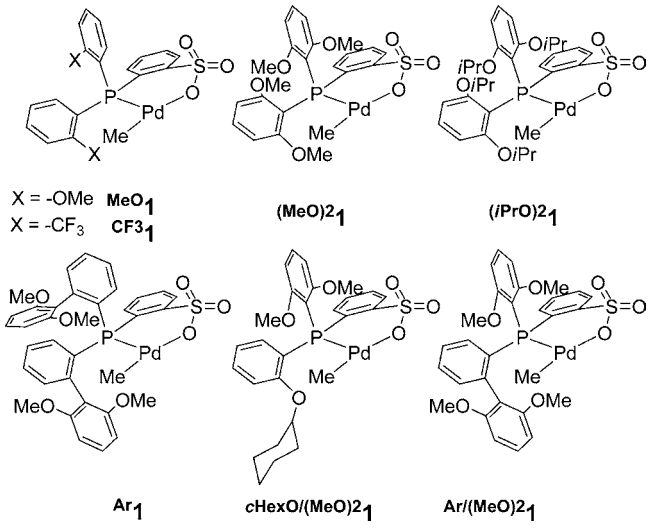

Figure 2. Phosphorus substitution patterns studied.

including the previously reported compounds ^{MeO}**1-L**, $^{(MeO)2}$**1-L**, and ^{Ar}**1-L**.[13,30,31] Commonly, the [(P^O)PdMe] fragment was generated in situ by halide abstraction from the cation-bridged complexes [{(^{X}**1-Cl**)-μ-M}$_n$] for insertion studies. For synthetic procedures and full characterization of all compounds, see the Supporting Information.

The crystal structures of $^{Ar/(MeO)2}$**1-lut** and $^{cHexO/(MeO)2}$**1-py** both show a square-planar geometry around the palladium center, with the methyl group trans to the sulfonate group, as observed generally for (P^O)PdMe complexes (Figure 3).

For the asymmetric complexes, a racemic 1:1 mixture of the two configurations at the phosphorus (*R*/*S*) is found. In $^{cHexO/(MeO)2}$**1-lut**, the double MeO-substituted aryl moiety is placed in the pseudoequatorial and the cyclohexyloxy-substituted aryl moiety in the pseudoaxial position, with the cyclohexyl-group aligned away from the Pd-center. In contrast, in $^{Ar/(MeO)2}$**1-py** the double MeO-substituted aryl moiety at phosphorus is arranged in the pseudoaxial position. The axial/equatorial alignment of the substituents does not depend on the configuration at the phosphorus atom (*R*/*S*), and the substituents determine the configuration of the (P^O) chelates in the solid state. Here, the more constrained substituent is always located in the less crowded pseudoequatorial ring-position. Consequently, the steric bulk of the substituents increased from 2-*c*HexOC$_6$H$_4$- to 2,6-(MeO)$_2$C$_6$H$_3$ to 2-(2′,6′-(MeO)$_2$C$_6$H$_3$)C$_6$H$_4$, and the $^{Ar/(MeO)2}$**1** fragment is substantially more crowded than the $^{cHexO/(MeO)2}$**1** fragment. This is also indicated by shorter distances of the aryl substituents to the Pd−Me in $^{Ar/(MeO)2}$**1-py** ($^{Ar/(MeO)2}$**1-py**, C(1)−C(8) = 3.138(6), C(1)−O(7) = 3.017(5) versus $^{cHexO/(MeO)2}$**1-lut**, C(1)−C(20) = 3.242(5), C(1)−C(9) = 3.527(5); cf., Supporting Information).

Analysis of Complex Flexibility. An essential point for this study is the analysis of the structure and possible motions of the (P^O)Pd system, as well as the time scale of such motions.[32−34] The (P^O)PdMe complex is capable of at least two independent motions, which can have a significant influence on the surrounding of the active center: A ring flip of the six-membered chelate formed by coordination of the bidentate ligand to the palladium center, and a rotation of the two non−chelating P-bound aryl moieties around the P−C bond (Figure 4). A comparison of all available X-ray structures

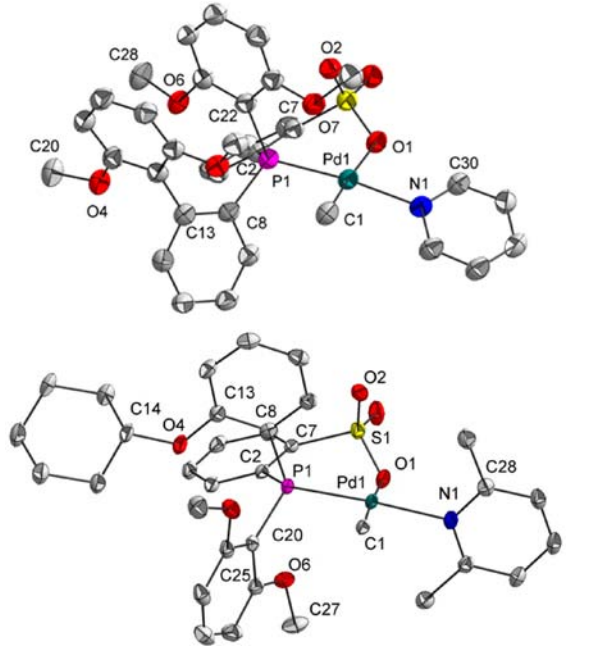

Figure 3. Solid-state structure of $^{Ar/(MeO)2}$**1-py** (top) and of $^{cHexO/(MeO)2}$**1-lut**. Ellipsoids represent 50% probability. Hydrogen atoms are omitted for clarity.

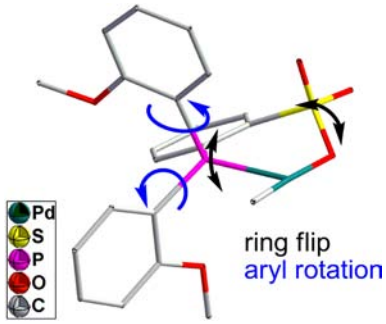

Figure 4. Observed molecular motions of (P^O)Pd complexes (fragment shown extracted from the X-ray structure of ^{MeO}**1**-OPBu$_3$).[43]

exhibiting the (P^O)Pd motif revealed that in nearly all cases a boatlike ring configuration is adopted by the six-membered (P^O)Pd chelates (for a detailed discussion, see the Supporting Information).[15,16,27,31,32,34−43] These chelate possess chirality and exist in two enantiomeric forms, which are also commonly found in the X-ray structures (cf., Supporting Information Figure S3). The phosphorus and the sulfur atom are situated at the ends of a boatlike conformation, which can flip from above to below the plane created by the other ring atoms (Figure 4). If this motion is fast as compared to monomer insertion, it scrambles the steric information, thus preventing a possible stereocontrol (vide infra).

Arylphosphinesulfonato ligands resemble an Ar$_3$ZX structure (here, X = lone pair, or H in the free ligand phosphonium tautomer), where all four ligands are arranged approximately tetrahedrally around the central atom Z. Because of a uniform

dx.doi.org/10.1021/ja3101787 | J. Am. Chem. Soc. 2013, 135, 1026−1036

aryl twist, these molecules show a helical configuration implying axial chirality (*P* or *M*).[44] As a result of the ortho substitution of the aryl moieties, various stereoisomeric configurations can be adopted. Experimentally only two different arrangements, exo_3 and exo_2, have been observed for (P^O)PdMe complexes: In the exo_3-configuration, all ortho substituents are situated on the same side as the central phosphorus above a plane defined by the three aryl carbons bound to phosphorus. In the exo_2-configuration, one of the ortho-substituents is situated underneath this plane (Figure 5).

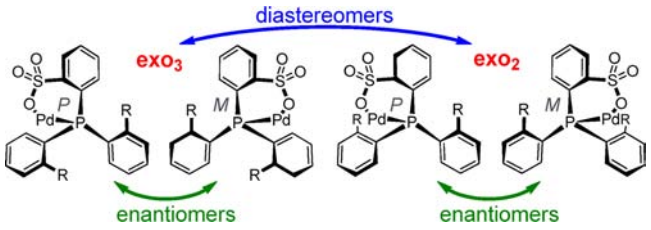

Figure 5. Helical chirality (P,M) as found for Ar_3ZX motifs and additional diastereomers for the case of ortho substitution of the aryl rings for [(P^O)PdMe] complexes.

The exo_2 configuration is observed for all [^{MeO}(P^O)PdMe(L)] structures.[16,27,30,32,38−40,43] Sterically more demanding aryl moieties such as $-C_6H_4Et$, $-C_6H_4[2,6\text{-}(MeO)_2C_6H_3]$, and 1-methoxynaphatalene generally favor the sterically less encumbered exo_3 configuration.[14,30,32,33] Consequently, a rigid configuration of the P-bound aryl moieties results in a stereocenter and may allow for a stereocontrol. Interconversion of the different isomers is only possible by correlated rotations of the aryl substituents.[45]

Dynamic NMR Studies. With regard to a stereoselection in catalysis, the dynamics in solution are relevant. Temperature-dependent NMR studies for the free ligands as well as for the complexes ^{X}**1** (generated in situ by chloride abstraction from [{(^{X}**1**-**Cl**)-μ-M}$_n$], cf., Supporting Information) revealed that only one dynamic process is observable in the temperature range from −90 to 130 °C. This is in line with related studies for ^{MeO}**1-py**, ^{Et}**1-py**, and ^{Ar}**1-py**.[32,34] It is assumed that an aryl rotation and not a ring flip process is observed in the NMR studies. This is based on the facts that, first, the non chelated free ligands (P^O)H and their respective salts (P^O)Na show a similar process.[46] Further, the freezing of molecular motions leads to an inequivalence of the aryl substituents, and the resonances in the ^{1}H NMR split. These new resonances provide further insights into the active process. In general, it is found here that the pair of corresponding ortho-aryl protons experiences the largest shift difference, whereas the para proton resonances remain nearly unchanged (cf., Supporting Information Figure S9). This is in line with an aryl rotation process, where the para-protons are within the axis of rotation. In contrast, a ring flip should have more pronounced influence on these para-protons.[47] For the asymmetric compound, $^{Ar/(MeO)2}$**1** formation of two diastereomers is observed at low temperature. The formation of diastereomers can be related to the combination of the permanent asymmetric center at phosphorus with the stereocenter derived at low temperature due to a fixed conformation (Figure S10, cf., Supporting Information for a detailed discussion, Figures S11−S30).

To gain deeper insights into the energetic barriers of the observed processes, dynamic NMR studies of the ligands ^{X}**(P^O)H** and the corresponding complexes were performed. Rate constants at variable temperatures were determined by a full line shape analysis, and an Eyring plot yielded $\Delta H^{\ddagger}$ and $\Delta S^{\ddagger}$, respectively (Table 1, cf., Supporting Information Figures S37−S48). For a comparison $\Delta G^{\ddagger}_{Tc}$ (at the coalescence temperature T_c) was calculated from $\Delta H^{\ddagger}$ and $\Delta S^{\ddagger}$, and also derived independently from the distance of the resonances in the slow exchange region ($\Delta\nu$) according to $k_c = \pi \times \Delta\nu/\sqrt{2}$ and $\Delta G^{\ddagger}_{Tc} = 19.14 \times T_c(10.32 + \log(T_c/k_c))$ J mol^{-1}.[48] The latter relationship was also used for determination of $\Delta G^{\ddagger}_{Tc}$ when line shape analysis was not applicable, as was the case for most of the ^{X}**(P^O)H** compounds.

The $\Delta G^{\ddagger}_{Tc}$ values obtained by the two different approaches agree well, and the comparison of $\Delta G^{\ddagger}_{Tc}$ for ^{MeO}**1** ($\Delta G^{\ddagger}_{Tc}$ = 44 kJ/mol, T_c = −50 °C, Table 1) determined for the MeO-groups nicely fits with the value determined by Jordan et al. for ^{MeO}**1-py** ($\Delta G^{\ddagger}_{Tc}$ = 44 kJ/mol, T_c = −50 °C).[32] A comparison of the different ligands reveals that for the protonated ligands ^{X}**(P^O)H** the rotational barrier increases with the steric bulk: MeO < CF_3 ≈ Ar.[49] The rotational barriers for complexes ^{X}**1** are always at least 10 kJ/mol higher than for the free ligands ^{X}**(P^O)H**. The highest barriers were found for ^{CF3}**1** for which even at 130 °C no fast interconversion was observed ($\Delta G^{\ddagger}_{Tc}$ > 76 kJ/mol). Because for ^{Et}**1** also a higher barrier was observed ($\Delta G^{\ddagger}_{Tc}$ = 64 kJ/mol)[32] in comparison to ^{MeO}**1** ($\Delta G^{\ddagger}_{Tc}$ = 44 kJ/mol), it appears that small changes in the β-position of the

Table 1. Results of Line Shape Analysis and Derived Energy Barriers for Various (P^O)Ligands and (P^O)PdMe Complexes

compound	resonance	T_c [°C]	$\Delta H^{\ddagger a}$ [kJ/mol]	$\Delta S^{\ddagger a}$ [kJ/mol]	$\Delta G^{\ddagger}_{Tc}$ [kJ/mol]^b/ [kJ/mol]^c
^{MeO}**(P^O)H**	−OMe	≪−90			<35[d]
^{MeO}**1**	−OMe	−50	39(1)	−17(4)	43(2)/44
^{CF3}**(P^O)H**	$-CF_3$	25			−/59
^{CF3}**1**	$-CF_3$	>130			>76[e]
^{Ar}**(P^O)H**	−OMe	20			−/59
^{Ar}**1**	−OMe	−43	46(2)	5(9)	45(3)/46
$^{Ar/(MeO)2}$**(P^O)H**	−OMe	−10			−/52[f]
$^{Ar/(MeO)2}$**(P^O)H**	P	≪−90			<35[d]
$^{Ar/(MeO)2}$**(P^O)Na**	P	−58	34(1)	−15(7)	38(3)/39[g]
$^{Ar/(MeO)2}$**1**	PdMe	25	48(1)	−27(1)	56(1)/59[g]

[a]Determined from Eyring plot. [b]Calculated from $\Delta G^{\ddagger} = \Delta H^{\ddagger} - T \times \Delta S^{\ddagger}$. [c]Calculated from $k_c = \pi\Delta\nu/\sqrt{2}$ and $\Delta G^{\ddagger}_{Tc} = 19.14 \times T_c(10.32 + \log(T_c/k_c))$ J mol^{-1}. [d]No hindered rotation observed down to −90 °C. [e]No coalescence observed up to 130 °C. [f]No formation of diastereomers observed, only rotation of 2,6-$(OMe)_2C_6H_3$− is hindered, and a process different from that for the corresponding sodium salt and complex occurs. [g]Formation of diastereomers observed.

dx.doi.org/10.1021/ja3101787 | J. Am. Chem. Soc. 2013, 135, 1026−1036

ortho substituents (O*Me* vs CH_2*Me* vs CF_3) can have a significant impact on the rotational barriers. The increase of the rotational barriers of around 10−20 kJ/mol upon coordination of the free ligands to a Pd-center agrees with previous observations on arylphosphine complexes (cf., Supporting Information for a detailed discussion). However, for the very bulky −C_6H_4(2,6-$(OMe)_2C_6H_3$) substituent, barriers for the complex ^{Ar}**1** are significantly lower than for the free ligand ($\Delta G^{\ddagger}_{Tc\text{-}Ar1}$ = 46 kJ/mol vs $\Delta G^{\ddagger}_{Tc\text{-}Ar(P\text{^}O)H}$ = 59 kJ/mol). For the asymmetric compounds, the formation of diastereomers is observed for $^{Ar/(MeO)2}$**(P^O)Na** and $^{Ar/(MeO)2}$**1** with a higher barrier for the complex ($\Delta G^{\ddagger}_{Tc\text{-}Ar/(MeO)2(P\text{^}O)Na}$ = 39 kJ/mol vs $\Delta G^{\ddagger}_{Tc\text{-}Ar/(MeO)21}$ = 59 kJ/mol).[50]

In conclusion, of the two motional processes affecting stereoselectivity, the aryl rotation possesses the significantly higher barriers in the range of 40−60 kJ/mol, whereas the ring flip process could not be observed in the accessible temperature range and must exhibit barriers always below ca. 35 kJ/mol. The observed barriers and corresponding coalescence temperatures are low in comparison to the temperatures required for an effective insertion reaction and polymerization, 60−90 °C. Only ^{CF3}**1** is an exception. Thus, in general the ligand framework must be regarded as conformationally fluxional.[47]

Stereoselectivity of MA Insertion. The reaction of the dimeric precursor [{(^{MeO}**1-Cl**)-μ-Na}$_2$] with $AgBF_4$ in the presence of MA in dichloromethane at 60 °C in a sealed tube affords the two diastereomeric products of the consecutive MA insertion into the Pd−Me bond ^{MeO}**3**$_{MA\text{-}rac}$ and ^{MeO}**3**$_{MA\text{-}meso}$ up to a 2:1 ratio (Figure 6).[51] This ratio was confirmed by ^{1}H, ^{31}P

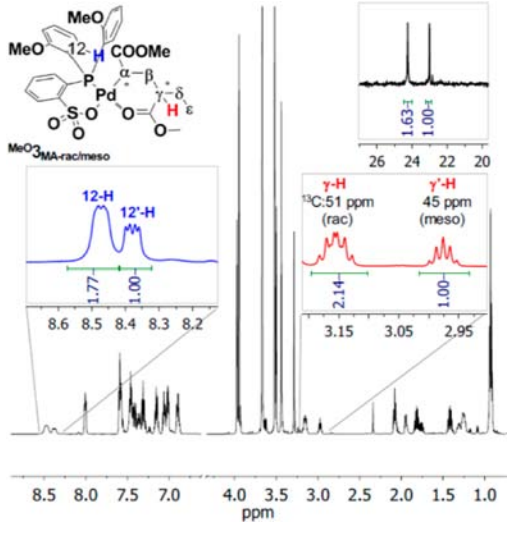

Figure 6. ^{1}H NMR spectrum of ^{MeO}**3**$_{MA}$ (600 MHz, CD_2Cl_2, 25 °C; inset ^{31}P NMR, 168 MHz). Insets: NMR resonances relevant for determination of stereoselectivity.[16]

NMR, as well as X-ray crystallography.[16,51] In the solid state, the aryl moieties adopt an exo$_2$ conformation. Because of the chirality of the chelate formed by the inserted MA, the anisyl moieties of the ligand are diastereotopic in ^{MeO}**3** and can be distinguished by NMR. An additional hindered rotation of these groups is unlikely, because it would lead to an additional stereocenter and hence the observance of four diastereomers for ^{MeO}**3**. A qualitative temperature-dependent NMR study reveals that up to 120 °C no intramolecular interconversion is detectable, but that additional diastereomers are observed at low temperature. The coalescence temperature for the MeO-resonances is in the same range as for ^{MeO}**1**, indicating that rotational barriers are roughly similar and consequently that the steric flexibility of the ligand is probably unchanged during an oligomerization process upon chain growth (cf., Supporting Information Figures S31−S33).

For a systematic investigation of stereoselectivity with different catalysts, a rapid and broad analysis protocol is essential. The formation of the two diastereomeric complexes ^{X}**3**$_{MA\text{-}meso}$ and ^{X}**3**$_{MA\text{-}rac}$ allows for a screening of stereoselectivity for the first two insertions, as these compounds are rather stable also in solution ($t_{1/2}$ > 3h) and the ratio of diastereomers can be analyzed by NMR spectroscopy (Figure 6). Analyzing the chelate formed by the MA insertion, the diastereomeric methine groups at Cγ and Cγ' in ^{MeO}**3**$_{MA\text{-}rac/meso}$ give rise to well separated proton resonances around 3 ppm (Figure 6). In addition, also the Cγ ^{13}C resonances show a pronounced shift difference (Cγ, 51 ppm; Cγ', 45 ppm), which allows for a transferable assignment of the meso/rac stereochemistry (vide infra). For a determination of stereoselectivity, also the low field shifted (in comparison to the starting material) resonances of the anisyl ortho protons 12-H of the (P^O) ligand at around 8.4 ppm can be drawn upon. In addition, the ^{31}P NMR spectrum and integrals can be utilized as well. Note that, due to underlying impurities, the exact ratios determined by integration of the different resonances pairs can deviate from each other.[51] For a rapid assignment of the crucial MA derived spin systems of new complexes, a combined ^{1}H, ^{1}H TOCSY/COSY-NMR analysis starting from the unique low field shifted γ-H resonances proved to be most effective.

Dependence of Stereoselectivity on Temperature. For an effective homopolymerization of polar monomers, temperatures between 60 and 90 °C are generally required.[14,16] Hence, the influence of temperature on the stereoselectivity of the consecutive MA insertion into ^{MeO}**1** was studied at temperatures up to 95 °C. To a mixture of [{(^{MeO}**1-Cl**)-μ-Na}$_2$] and $AgBF_4$ in $C_2D_2Cl_4$ was added 20 equiv of MA, and the reaction mixture was kept at the corresponding temperature in an NMR tube. Reaction times are strongly dependent on the reaction temperature. Whereas consecutive insertion was completed within 20 min at 95 °C, at 60 °C 90 min and at 25 °C 24 h were required. Insertion at 4 °C was still not completed after a week, and solvents and monomer were removed at 0 °C and the remaining mixture of ^{MeO}**2**$_{MA}$ and ^{MeO}**3**$_{MA}$ was analyzed. The slow progress of reaction at 4 °C indicates that a further temperature decrease is not reasonable for the catalyst system ^{MeO}**1**. The insertion experiments clearly reveal that an influence of temperature on stereocontrol is negligible, and that the ratio of the stereoisomers is temperature-independent within experimental error (cf., Supporting Information Figures S49 and S50).

Dependence of Stereoselectivity on Steric Bulk of the Monomer. Because ^{MeO}**1** exhibits no permanent chiral center, and the above studies revealed a fast interconversion of conformers, methyl acrylate insertion is likely dominated by a chain-end stereocontrol mechanism as proposed previously.[16] To further analyze this issue, the influence of the monomers bulk on the stereoselectivity was studied. For this purpose, the insertion of MA, isopropyl acrylate (*i*PrA), and *tert*-butyl acrylate (*t*BuA) at 25 °C was compared under the same experimental conditions as described above. The comparison of the crude insertion products revealed that the steric bulk of the monomer primarily influences the regioselectivity.

dx.doi.org/10.1021/ja3101787 | J. Am. Chem. Soc. 2013, 135, 1026−1036

Table 2. Rate Constants of Insertion and β-H Elimination, and Stereoselectivity for Various Phosphinesulfonato Ligands[a]

entry	compound	k_{first} [10^{-3} s^{-1}]	regioselectivity first insertion $^{X}2_{2,1}$: $^{X}2_{1,2}$	stereoselectivity first insertion	k_{second} [10^{-5} s^{-1}]	stereoselectivity second insertion (rac:meso)
2-1	^{MeO}**1**	3.2	>15:1		9	2:1
2-2	^{CF3}**1**	4.8	4:1		43	2:1
2-3	$^{(MeO)2}$**1**	1.3	>30:1		4	1:1
2-4	$^{(iPrO)2}$**1**	3.4	7:1		~1[b]	1:1
2-5	^{Ar}**1**	~1[b]	1:1	*c*	*d*	*d*
2-6	$^{Ar/(MeO)2}$**1**	3	2:1	6:1	6	3:1
2-7	$^{cHexO/(MeO)2}$**1**	3	6:1	~1:1[e]	5	1:1

[a]Conditions: [Pd] = 0.02 mol L^{-1}, 1.1 equiv $AgBF_4$, Pd:MA ~ 1:15, solvent: CD_2Cl_2, T = 25 °C. [b]Estimate, exact determination not possible. [c]A 2:1 ratio of two ^{Ar}**2**$_{MA-2,1}$ products is found. However, diastereomer formation is probably due to hindered aryl rotation in ^{Ar}**2**, and interconversion of the isomers is possible. [d]No consecutive insertion observed. [e]Additional 2,1-insertion products observed, clear assignment not possible.

For MA only a trace amount of the 1,2 insertion product ^{MeO}**2**$_{MA-1,2}$ was observed, whereas for *t*BuA a ratio ^{MeO}**2**$_{tBuA-1,2}$:^{MeO}**2**$_{tBuA-2,1}$ of ~1:5 is found. For *i*PrA, the portion of 1,2 insertion product cannot be determined due to overlapping resonances, but it appears to be similar to that for *t*BuA. Concerning the stereoselectivity of the consecutive insertion, an unexpected trend was found: With increasing steric bulk of the monomer, stereoselection is reduced, as concluded from the integration of the ortho aryl protons (cf., Supporting Information Figures S51 and S52). The rac:meso ratio decreases from 2.2:1 for ^{MeO}**3**$_{MA}$ over 1.5:1 for ^{MeO}**3**$_{iPrA}$ to 1.1:1 for ^{MeO}**3**$_{tBuA}$. Hence, it appears here that chain-end stereocontrol and any enantiomorphic site stereocontrol work uncooperatively in different directions.

Influence of Ligand Structure and Complex Conformation on Stereoselectivity. To shed light on the influence of the complex structure on the insertion behavior, the reaction of ^{MeO}**1**, ^{CF3}**1**, $^{(MeO)2}$**1**, $^{(iPrO)2}$**1**, ^{Ar}**1**, $^{Ar/(MeO)2}$**1**, and $^{cHexO/(MeO)2}$**1** (generated in situ from [{(^{X}**1-Cl**)-μ-M}$_n$]) with MA to the mono insertion products ^{X}**2**$_{MA}$ and the products of consecutive insertion ^{X}**3**$_{MA}$ were monitored over time by NMR spectroscopy (Scheme 1).

The regioselectivity in the first insertion is determined from the distribution of 1,2- to 2,1-insertion products ^{X}**2**$_{MA}$. The formation of the 1,2 insertion product is generally disadvantageous because the resulting five-membered chelates inhibit further insertions.[16] Regarding the first insertion, the influence of the phosphinesulfonato substitution pattern on the rate constant k_{first} is rather low for the complexes investigated, and cannot always be distinguished from electronic effects. By contrast, the steric bulk has a significant influence on the regioselectivity. Here, an increase of the constraints around the active center leads to a shift toward the 1,2 insertion product as illustrated, for example, by the shift of the 2,1:1,2 ratio from >15:1 for ^{MeO}**2**, over 4:1 for ^{CF3}**2**, to ~1:1 for ^{Ar}**2** (Table 2). A complete inversion of regiochemistry to 1,2 insertion versus the 2,1 insertion of ^{MeO}**1** has been observed previously for the very bulky (κ^2-*P*,*O*)-diazaphospholidine-sulfonato ligands, which is due to a destabilization of the 2,1-insertion transition states.[40]

For the asymmetric substituted compounds $^{Ar/(MeO)2}$**1** and $^{cHexO/(MeO)2}$**1**, several 2,1 insertion products are formed due to the permanent stereo center at phosphorus. A selectivity of 6:1 was found for $^{Ar/(MeO)2}$**1**, indicating an effective enantiomorphic site stereocontrol. For $^{cHexO/(MeO)2}$**2**, analysis is complicated due to formation of additional species, probably due to hindered rotation, but selectivity for the first insertion is roughly 1:1. Consequently, the exchange of a *c*HexOC$_6$H$_4$ substituent by a 2-{2′,6′-(MeO)$_2$C$_6$H$_3$}C$_6$H$_4$ moiety significantly increases selectivity. This corresponds with the increased steric bulk at the Pd–Me for $^{Ar/(MeO)2}$**1** in the solid state and is reflected in the different alignment (pseudoaxial/equatorial) of the second 2,6-(MeO)$_2$C$_6$H$_3$ substituent in the X-ray structures for theses two complexes (Figure 3).

The insertion rates for the consecutive MA insertion are 1–2 orders of magnitude lower than for the first insertion. This is due to a slower insertion into an α-substituted carbyl versus insertion into a methyl group, and due to chelating coordination of the carbonyl group of the incorporated acrylate unit, which competes with the incoming monomer.[16,43] Other than for the first insertion, a more pronounced influence of the steric bulk of the ligand on the rate constant k_{second} is found. As expected, k_{second} decreases with steric bulk as illustrated by comparison of ^{MeO}**1** (k_{second} = 9 × 10^{-5} s^{-1}) and $^{Ar/(MeO)2}$**1** (k_{second} = 6 × 10^{-5} s^{-1}). Introduction of a second 2,6-(MeO)$_2$C$_6$H$_3$ substituent in ^{Ar}**1** even leads to a complete inhibition of the consecutive insertion (entry 2-1 vs 2-5 vs 2-6). That electronics can still dominate in the case of less pronounced differences in steric bulk becomes clear by considering that for ^{CF3}**1**, exhibiting the highest rotational barrier (vide supra), the consecutive insertion seems to be accelerated due to electronic effects leading to the highest rate constant k_{second} = 40 × 10^{-5} s^{-1} of all investigated complexes, whereas for the most electron-rich complex $^{(MeO)2}$**1** the insertion rate is significantly lower with k_{second} = 4 × 10^{-5} s^{-1} (compare entry 2-1 to 2-3).

The stereoselectivity for the symmetric complexes was determined from the product distribution after consecutive MA insertion to form ^{X}**3**$_{MA}$ (vide supra). A comparison of the MA insertion into ^{MeO}**1** with ^{CF3}**1** at room temperature reveals that the enhanced rotational barrier of the CF_3-substituted complex does not lead to a significant increase of selectivity (~2:1, Figure S53). In the complexes with C_{2v}-symmetric aryl moieties $^{(MeO)2}$**3**$_{MA}$ and $^{(iPrO)2}$**3**$_{MA}$, the selectivity is even diminished in comparison to the compounds with C_s-symmetric aryl moieties, again a substitution of the MeO-groups by the sterically more demanding *i*PrO-groups does not influence the selectivity significantly (Table 2, Figure S53). From the carbon shifts of the C_γ methine groups, an absolute assignment of stereochemistry is possible (vide supra). An increase of steric bulk leads to an equilibration of the rac:meso product ratio, which was also observed for an increase of monomer steric bulk (vide supra).

For the compounds $^{cHexO/(MeO)2}$**3**$_{MA}$ and $^{Ar/(MeO)2}$**3**$_{MA}$, analysis of the insertion products is more complex, because the presence of the permanent stereocenter at phosphorus leads to the formation of at least four diastereomers ^{X}**3**$_{MA}$. For

dx.doi.org/10.1021/ja3101787 | J. Am. Chem. Soc. 2013, 135, 1026–1036

$^{cHexO/(MeO)2}\mathbf{3}_{MA}$, all four diastereomers can be detected by ^{1}H, ^{1}H TOCSY-NMR analysis (cf., Supporting Information Figure S73). Integration of the γ-H methine proton yields a distribution of roughly 1:4:5:8. Assignment of the diastereomers to meso and rac species is possible by analysis of the ^{13}C NMR spectra, assuming that a similar chain configuration reflects in similar carbon shifts. Consequently, the C_γ-methine ^{1}H resonances of $^{cHexO/(MeO)2}\mathbf{3}_{MA}$ at 3.27 (^{13}C: 44 ppm) and 2.82 (^{13}C: 45 ppm) can be assigned to the meso isomers and the resonances at 3.21 (^{13}C: 51 ppm) and 3.00 ppm (^{13}C: 52 ppm) to the rac isomers, corresponding to a rac:meso selectivity of ~1:1. For $^{Ar/(MeO)2}\mathbf{3}_{MA}$, analysis is complicated by overlapping resonances, but the insertion products evidently are formed in rather similar proportions. In this case, the α-H methine resonances integrals were employed (Figure 7).

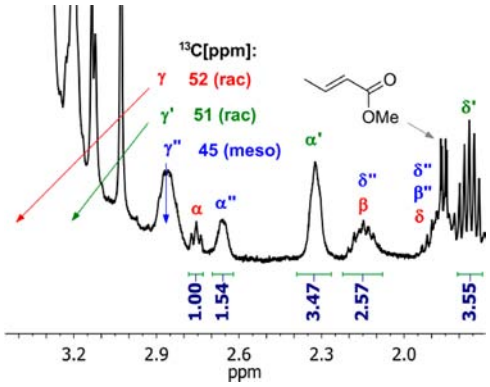

Figure 7. Distribution (^{1}H NMR, 400 MHz, CD_2Cl_2) of the three diastereomers of $^{Ar/(MeO)2}\mathbf{3}_{MA}$ (for a complete assignment of the spin systems, see Figures S70 and S71).

Assignment of the spin systems by ^{1}H, ^{1}H TOCSY and ^{1}H, ^{13}C gHSQC experiments clearly shows the formation of only three main diastereomers and yields a rac:meso distribution of 3:1. Thus, the high selectivity for the first insertion (6:1) is diminished for the consecutive insertion, indicating that the possible chain-end control, which becomes active from the second insertion on, is opposite to the enantiomorphic site stereocontrol, which controls the first insertion alone.

Computational Studies. To gain a deeper understanding of the dynamics, regio- and stereocontrol mechanisms in (P^O)PdMe complexes, alkyl acrylate insertion into the Pd–Me bond of $^{MeO}\mathbf{1}$, $^{(MeO)2}\mathbf{1}$, $^{Ar}\mathbf{1}$, and $^{Ar/(MeO)2}\mathbf{1}$ was studied by DFT (see the Supporting Information for computational details). Considering the limited selectivity achieved experimentally, the energy differences are expected to be rather low, almost within the error expected for this kind of calculation, and thus trends from the comparison of different systems are more indicative than the energy values specific to a single system.[52]

The established theoretical understanding of the insertion mechanism with (P^O)Pd catalysts is briefly summarized using insertion of MA into the Pd–Me bond of $^{MeO}\mathbf{1}$ as an example (Scheme 2).[16,27,28,40,53] The growing chain is always oriented trans to the sulfonate group in the initial species, and coordination of the monomer occurs cis to phosphorus as in $^{X}\mathbf{1}$-$\mathbf{MA}_{cis}$. The preferred pathway for insertion into the Pd–C bond proceeds through a Berry-pseudo rotation step that isomerizes $^{X}\mathbf{1}$-$\mathbf{MA}_{cis}$ to the less stable $^{X}\mathbf{1}$-$\mathbf{MA}_{trans}$ species. The 2,1-insertion of MA into the Pd–C bond of $^{X}\mathbf{1}$-$\mathbf{MA}_{trans}$ through

Scheme 2. MA Coordination and Insertion with $^{MeO}\mathbf{1}$[a]

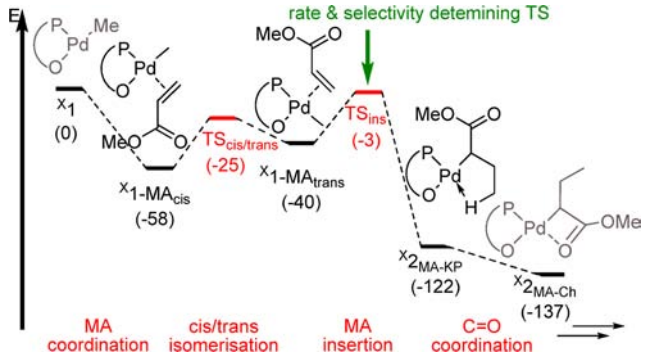

[a]Relative energies of the species are given in parentheses (kJ/mol; black, intermediates; red, transition states).[16]

transition state TS_{ins} leads to the γ-agostic stabilized kinetic product $^{X}\mathbf{2}_{MA\text{-}KP}$. The final insertion product is $^{X}\mathbf{2}_{MA\text{-}Ch}$, in which the carbonyl group of the inserted MA is coordinated to the metal center. The mechanism of further insertions is similar, the major difference being the nature of the starting and final complexes and their respective energy, due to the formation of 4- or 6-membered chelates after the first and the second insertion, respectively.

Site stereocontrol requires a permanent rigid chiral configuration on the time scale of insertion. Hence, for a symmetrically substituted phosphorus atom as in $^{MeO}\mathbf{1}$, $^{(MeO)2}\mathbf{1}$, and $^{Ar}\mathbf{1}$, at least a stable helical configuration at the phosphorus atom or a stable ring configuration is necessary. If ring flip and aryl rotation exhibit significantly lower barriers in comparison to insertion, the first MA insertion cannot be enantioselective. The corresponding transition states for ring flip (TS_{RF}) and aryl rotation (TS_{AR}) in the MA complexes $^{X}\mathbf{1}$-$\mathbf{MA}$ are compared to the transition state for the first 2,1-insertion (TS_{Ins}) in Table 3.

Table 3. Transition State Energies (kJ/mol) for MA Insertion into $^{X}\mathbf{1}$ and for Ring Flip and Aryl Rotation for $^{X}\mathbf{1}$-MA

compound	TS_{Ins}	ring flip-TS	aryl rotation-TS
$^{MeO}\mathbf{1}$	0	−49	−34
$^{(MeO)2}\mathbf{1}$	0	−51	−[b]
$^{Ar}\mathbf{1}$	0	−49	−14
$^{Ar/(MeO)2}\mathbf{1}^a$	0	−18	−5

[a]Configuration at phosphorus: (*R*). [b]Aryl rotation is not possible, because the MeO-groups inevitably collide in the corresponding TS.

The reported values indicate that TS_{ins} is higher in energy than TS_{AR} and TS_{RF} for $^{MeO}\mathbf{1}$ and $^{Ar}\mathbf{1}$, which indicates that here the first MA insertion is not stereoselective. Further, in agreement with the NMR studies, the energy barriers for aryl rotations are always at least 13 kJ/mol higher than the barriers for the ring flip and increase with the steric bulk of the nonchelating aryl moieties.[54] Considering that the ring flip is consistently calculated to be a low energy process, it is assumed to be generally rapid as compared to aryl rotation and acrylate insertion and is not further discussed in the following.

For the bulky $^{(MeO)2}\mathbf{1}$-$\mathbf{MA}$ system, rotation of the aryl groups is hampered because the MeO-groups inevitably collide in the corresponding TS_{AR} and the fixed chiral conformation (*P* or *M*) of the complex could in principle select between *re*- or *si*-MA insertion. However, analysis of the TS_{ins} geometry for a *P*

dx.doi.org/10.1021/ja3101787 | J. Am. Chem. Soc. 2013, 135, 1026–1036

configuration at the active site reveals no significant differences in the interaction between the two MA enantiofaces and the ligand, due to the high symmetry of the system (Figure 8). Consequently, the energy difference between the *re*- and *si*-MA TS_{Ins} is negligible (<1 kJ/mol).

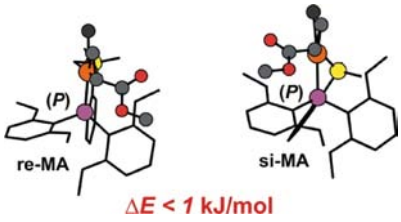

Figure 8. Transition states for *si*- and *re*-MA insertion into $^{(MeO)2}\mathbf{1}$ with a *P* helical configuration of the aromatic rings.

The asymmetric system $^{Ar/(MeO)2}\mathbf{1}$ exhibits a permanent stereocenter at the phosphorus and can in principle distinguish between the different MA enantiofaces even if molecular motions are fast. In fact, a significant energy difference ΔE_{stereo} = 11 kJ/mol between the two respective lowest energy transition states for acrylate insertion into the Pd−Me bond was found. In case of an *R* configuration at the phosphorus atom (which favors a *P* helical chirality), insertion of a *re*-MA is favored (Figure 9).

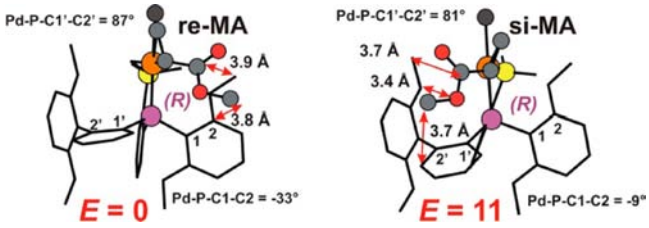

Figure 9. Transition states for *si*- and *re*-MA insertion into $^{Ar/(MeO)2}\mathbf{1}$ with a *P* helical configuration of the aromatic rings.

The calculated ΔE_{stereo} of 11 kJ/mol is in reasonable agreement with the experimental stereoselectivity ratio of 6:1. As depicted in Figure 9, the interaction between the 2,6-$(MeO)_2(C_6H_3)$-moiety and the monomer is responsible for the higher energy of the *si*-MA insertion into the Pd−Me bond of the $^{Ar/(MeO)2}\mathbf{1}$ complex with a *R* configuration at the phosphorus (shortest distances of 3.7 Å for *si*-MA as compared to 3.9 and 3.8 Å in the favored *re*-MA insertion).

The first MA insertion generates a chiral carbon atom directly bound to the metal center, with *re*- and *si*-MA insertion resulting in *R* and *S* configuration of the chiral carbon atom, respectively. Considering this, the second MA insertion differs from the first in that either an interaction of the chiral chain end with the ligand may force the catalytic site to assume a specific chiral conformation or the chiral chain itself may select between the monomer enantiofaces directly. Table 4 reports the calculated ΔE_{stereo} for the first two acrylate insertion steps. In agreement with experiments, the calculations indicate that the chiral chain end is unable to discriminate between the two MA enantiofaces, even in case of bulky ligands. Further, these results indicate that stereoselectivity due to direct interaction between the chiral growing chain and the monomer is negligible, which is reasonable considering that 2,1-insertion

Table 4. Stereo- and Regioselectivity for the First and the Second Acrylate Insertion into $^{X}\mathbf{1}$ (Energies in kJ/mol)

		ΔE_{stereo}		ΔE_{regio}	
compound	acrylate	first ins	second ins[a]	first ins[b]	second ins[d]
$^{MeO}\mathbf{1}$	MA		−1(1)[c]	9(10)[c]	27
$^{(MeO)2}\mathbf{1}$	MA	0	0	11	29
$^{Ar}\mathbf{1}$	MA		−1	0	14
$^{Ar/(MeO)2}\mathbf{1}$	MA	11	3	7	12
$^{MeO}\mathbf{1}$	*t*BuA		2	−2	11

[a]Positive numbers correspond to preference of the meso product $^{X}\mathbf{3}_{MA\text{-}meso}$. [b]Positive numbers correspond to preference of the 2,1 MA insertion product. [c]The values in parentheses are obtained with the ADF program and were reported previously.[16] [d]$\Delta E_{regio} = E_{2,1-1,2} - E_{2,1-2,1}$: positive numbers correspond to preference of $^{X}\mathbf{3}_{MA}$. Helical chirality for all compounds: (*P*).

places the functional group of the monomer away from the growing chain (Figure S75).

For the asymmetric system $^{Ar/(MeO)2}\mathbf{1}$, four different consecutive insertion products $^{Ar/(MeO)2}\mathbf{3}$ can be formed, due to the chirality at the phosphorus. The energy differences ΔE_{stereo} between the four transition states are reported in Table 5. In the first insertion, a *R* chain is preferentially generated from the most stable *re*-MA TS_{Ins} (Figure 9). For the second MA insertion, stereoselectivity is diminished. In detail, other than the NMR studies, the calculations indicate a slight preference for the meso isomer. The loss of enantiomorphic site control in favor of the *re*-MA enantioface in the second insertion step can be explained by steric interaction between the ethyl group of the chain and the ligand (Figure 10). The 2,6-$(MeO)_2(C_6H_3)$ moiety at the phosphorus is rotated in comparison to the TS_{ins} of the first *re*-MA insertion, and one of the methoxy groups is now arranged at a critical distance of only 3.5 Å from the monomer (dihedral angle θ (Pd−P−C1−C2): −33°(*re*-MA_{first}) vs −9°(*re*-MA_{second}); compare −9°(*si*-MA_{first}) vs −14°(*si*-MA_{second}); Figure 9 vs Figure 10). As a consequence, enantiomorphic site and chain end stereocontrols act in opposite directions for $^{Ar/(MeO)2}\mathbf{2}$ so that stereoselectivity in the second MA insertion is definitively lost. Calculations indicate that due to the flexibility of the system, the ligand evades the growing chain and any kind of stereoselectivity in the MA polymerization is prevented.

Because the production of defined tactic polymers does not only depend on stereoselectivity but also on regioregularity, and experiments showed that both insertion modes (1,2 and 2,1) are observable, at least for the first insertion, the influence of the ligand structure on regioselectivity was investigated. Here, the energy difference between the transition states for 2,1 and 1,2 monomer insertion was calculated for the first insertion with $^{X}\mathbf{1}_{MA}$ ($\Delta E_{regio,first}$, Table 4), as well as for MA insertion with $^{X}\mathbf{2}_{2,1\text{-}MA}$ ($\Delta E_{regio,second}$, Table 4). In contrast, consecutive 1,2-insertion into $^{X}\mathbf{2}_{1,2\text{-}MA}$ is energetically not favorable because of steric interaction between the monomer and the 1,2 chain end, and was also not observed experimentally so far.[55]

As expected and in agreement with previous work, calculations show that the shift from the electronically favored 2,1-transition state to the less sterically constrained 1,2-transition state depends on the structure of the ligand and the size of the monomer.[40] The 1,2-transition state becomes more favored by increasing either the size of the P-aryl substituents of the chelating ligands from $^{MeO}\mathbf{1}$ ($\Delta E_{regio,first}$ = 9 kJ/mol) to $^{Ar/(MeO)2}\mathbf{1}$ ($\Delta E_{regio,first}$ = 7 kJ/mol) to $^{Ar}\mathbf{1}$ ($\Delta E_{regio,first}$

dx.doi.org/10.1021/ja3101787 | J. Am. Chem. Soc. 2013, 135, 1026−1036

Table 5. ΔE_{stereo} (kJ/mol) for All Transition States to the Insertion Products of the First and Second MA Insertions into $^{Ar/(MeO)2}$**1** with a (*R*) Configuration at the Phosphorus and *P* Helical Configuration of the Aromatic Rings

	$^{Ar/(MeO)2}$**1**					
	MA first insertion (2,1)		MA second insertion (2,1; 2,1)			
	re	*si*	*re*/*R*	*si*/*R*	*re*/*S*	*si*/*S*
ΔE_{stereo}	0	11	0	3	10	4
product	$^{Ar/(MeO)2}$**2**$_{MA-2,1}$	$^{Ar/(MeO)2}$**2**$_{MA-2,1}$′	$^{Ar/(MeO)2}$**3**$_{MA-meso}$	$^{Ar/(MeO)2}$**3**$_{MA-rac}$	$^{Ar/(MeO)2}$**3**$_{MA-rac}$′	$^{Ar/(MeO)2}$**3**$_{MA-meso}$′

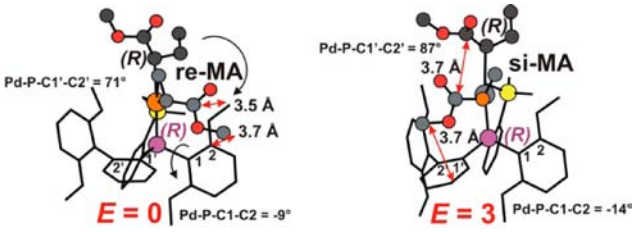

Figure 10. Transition states for the MA insertion into $^{Ar/(MeO)2}$**2**$_{MA}$ to $^{Ar/(MeO)2}$**3**$_{MA-meso}$ (left) and $^{Ar/(MeO)2}$**3**$_{MA-rac}$ (right); *R* configuration at the phosphorus atom and *P* helical configuration of the aromatic rings.

= 0 kJ/mol) or the size of the monomer from MA to *t*BuA (^{MeO}**1** $\Delta E_{regio,first}$ = −2 kJ/mol). The 2,1- and 1,2-transition states for the first insertion of MA into ^{Ar}**1** and of *t*BuA into ^{MeO}**1** are compared in Figure 11. In both cases, regioselectivity

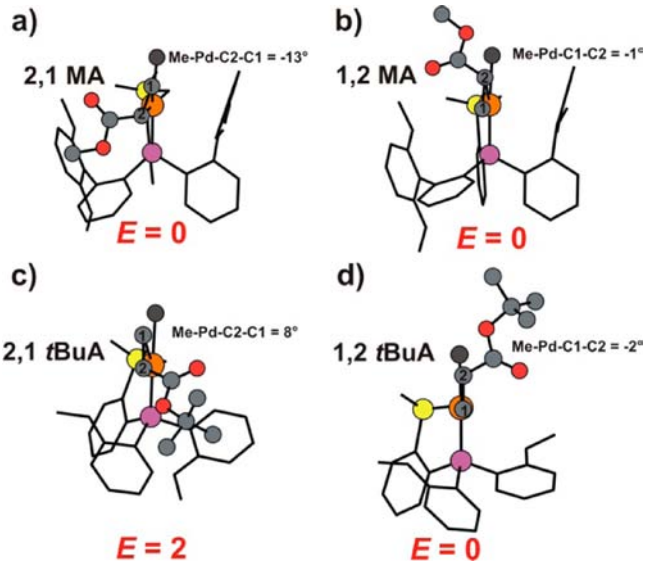

Figure 11. Regioselectivity of MA insertion into ^{Ar}**1** (a,b) and of *t*BuA insertion into ^{MeO}**1** (c,d).

is completely lost ($\Delta E_{regio,first}$ = 0−2 kJ/mol). As reported previously, the decrease of regioselectivity can be rationalized by an analysis of the deviation from planarity of the four center Cossée−Arlman-like transition state that increases by increasing the sterical pressure of the system.[40] The extent of this deviation can be estimated by comparing the Me−Pd−C1−C2 dihedral angles for the 2,1-transition states in Figure 11 with the value for the 2,1-transition state for ^{MeO}**1** reported previously.[40] The deviation from 0° for insertion into ^{MeO}**1** increases from MA insertion (−4°)[40] to *t*BuA insertion (8°) (Figure 11). Conclusively, in agreement with the experimental observations, an increase of steric constrains via the phosphinesulfonato ligand or the monomer decreases the regioselectivity of the insertion.

CONCLUSIONS AND OUTLOOK

As has been understood in the past few years, palladium complexes with unsymmetrical, hard/soft chelating phosphinesulfonato ligands are unique in allowing for ethylene copolymerization with a large range of polar vinyl monomers and even enable insertion homopolymerization of acrylates.

An analysis of intramolecular interconversion processes showed that the ligand framework is rather flexible and undergoes several transformations including an aryl rotation in a propeller-like conformation environment and a ring flip process of the six-membered (P^O)Pd chelate. The highest barriers $\Delta G^{\ddagger}$ of these processes, of the aryl rotation, were found to add up to 40−60 kJ/mol for the methyl complexes (^{X}**1**). Theoretical calculations revealed that also for the monomer-coordinated complexes ^{X}**1-MA** the transition states for the intramolecular motions are significantly lower than the insertion transition states. An exception was found for systems that bear double ortho substituted aryl moieties at phosphorus. Here, an aryl rotation is inhibited, but still the transition states for both enantiofaces of the monomer are rather similar due to the symmetry of the ligand.

Conclusively, a permanent chiral center at phosphorus by asymmetric substitution is a prerequisite for a stereocontrol of insertion. This concept is underlined by the experimental observation of a 6:1 stereoselectivity in the first insertion with the asymmetric complex $^{Ar/(MeO)2}$**1**. For the consecutive insertions, stereocontrol is reduced. The theoretical calculations are in line with these results and indicate that the high flexibility of the ligand is responsible for the loss of stereocontrol. The ligand evades the growing chain and transition states are equilibrated for the consecutive insertion, because site stereocontrol and chain end stereocontrol work uncooperatively. NMR-insertion studies with ^{MeO}**1** showed that within the accessible temperature range, stereoselectivity cannot be influenced by temperature. Further, insertion studies of monomers with variable steric bulk (MA, *i*PrA, *t*BuA) revealed that stereocontrol decreases with increasing steric bulk, which indicates that also in this case chain end stereocontrol and enantiomorphic site stereocontrol work together uncooperatively.

Beyond the effects on stereocontrol, a clear relation between steric bulk and the regioselectivity of insertion was found, such that increased steric bulk in the ligand or in the monomer leads to a shift from the desired 2,1- to the 1,2-insertion mode. The resulting 1,2-insertion products are not amenable to further insertions due to the stability of the five-membered chelate formed by coordination of the carbonyl group of the incorporated acrylate. Theoretical considerations clearly show that deviation from the planarity of the four center Cossée−Arlman-like transition state increases the sterical pressure of the

dx.doi.org/10.1021/ja3101787 | J. Am. Chem. Soc. 2013, 135, 1026−1036

system and results in energetically similar 1,2- and 2,1-insertion transition states. That is, site differentiation by extreme steric bulk is not a feasible approach to tactic polymers because the regioregularity is lost. In addition, the insertion studies also disclosed an intrinsic problem of these catalysts: Increase of steric bulk always leads to a reduction of the acrylate insertion rates, and thus hinders chain growth. This culminates in a complete suppression of consecutive insertions for ^{Ar}**1**.

Further Concepts. These limitations understood it is also evident that there is a "window" of intermediate steric bulk, which allows stereoselection without compromising regioregularity. In more general terms, it is remarkable that any stereoselection at all is possible in the open environment of the hard/soft unsymmetric phosphinesulfonato ligand (Figure 1). One decisive feature appears to be the insertion from the alkyl-olefin complex with the π-bound acrylate in cis-position to the P-donor. This allows for influencing the stereoselectivity of the insertion step via the P-substituents. With the concept of an unsymmetric substitution, stereocontrol was realized. A reduction of flexibility in such asymmetric complexes appears a possible approach toward stereoselective polymerization. Reduction of flexibility has already been shown to be possible by a double ortho substitution of the aryl moieties at phosphorus. However, a more effective concept may be the introduction of a rigid spacer between the two different aryl moieties (Figure 12). This could further allow one to place the

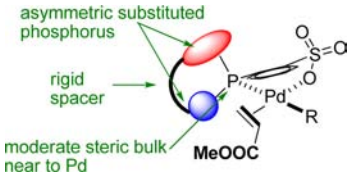

Figure 12. Concepts toward stereoselective catalysts.

chiral information in the spacer, which might reduce steric bulk at the active center. Preliminary analysis of the transition state configuration reveals that for a rigid aryl configuration presumably no large difference in size between the substituents at the phosphorus is required, which again could help to keep the steric bulk at the active center moderate.

Note that in parallel to this work, Nozaki et al. communicated that (P^O)PdMe complexes with asymmetric substitution at phosphorus like $^{Ar/H}$**1** are capable of asymmetric copolymerization of CO with polar monomers. In this case, the copolymerization with CO introduces a nonchiral CO-spacer between the chiral side chains. This apparently advantageously reduces a chain end stereocontrol, which in our work counteracts the enantiomorphic site stereocontrol of the homoinsertions.[56]

■ ASSOCIATED CONTENT

Supporting Information

Text, tables, figures, and CIF files giving detailed experimental procedures and analytical data, structural diagrams, selected bond lengths and angles, and crystallographic data/processing parameters for all structures. This material is available free of charge via the Internet at http://pubs.acs.org.

■ AUTHOR INFORMATION

Corresponding Author

stefan.mecking@uni-konstanz.de; lcaporaso@unisa.it

Notes

The authors declare no competing financial interest.

■ ACKNOWLEDGMENTS

This work was financially supported by the DFG (Me 1388/10). B.N. acknowledges support by the state of Baden-Württemberg by a Landesgraduiertenförderung-Stipend. We thank Anna-Lena Steck for high resolution ESI−MS measurements, Thomas Wiedemann for participation in this research as a part of his undergraduate studies, Inigo Göttker-Schnetmann for fruitful discussions, and the HPC team of Enea for use of the ENEA-GRID and the HPC facilities CRESCO in Portici, Italy.

■ REFERENCES

(1) Baugh, L. S.; Canich, J. M. *Stereoselective Polymerization with Single-Site Catalysts*; CRC Press: London, 2008.
(2) Matsuzaki, K.; Uryu, T.; Ishida, A.; Ohki, T.; Takeuchi, M. *J. Polym. Sci., Part A-1: Polym. Chem.* **1967**, *5*, 2167−2177.
(3) Liu, W.; Nakano, T.; Okamoto, Y. *Polym. J.* **1999**, *31*, 479−481.
(4) Deng, H.; Soga, K. *Macromolecules* **1996**, *29*, 1847−1848.
(5) Porter, N. A.; Allen, T. R.; Breyer, R. A. *J. Am. Chem. Soc.* **1992**, *114*, 7676−7683.
(6) Liu, W.; Nakano, T.; Okamoto, Y. *Polymer* **2000**, *41*, 4467−4472.
(7) Matsuzaki, K.; Uryu, T.; Kanai, T.; Hosonuma, K.; Matsubara, T.; Tachikawa, H.; Yamada, M.; Okuzono, S. *Makromol. Chem.* **1977**, *178*, 11−17.
(8) Brintzinger, H.-H.; Fischer, D.; Mülhaupt, R.; Rieger, B.; Waymouth, R. *Angew. Chem., Int. Ed. Engl.* **1995**, *34*, 1143−1170.
(9) Resconi, L.; Cavallo, L.; Fait, A.; Piemontesi, F. *Chem. Rev.* **2000**, *100*, 1253−1346.
(10) Johnson, L. K.; Mecking, S.; Brookhart, M. *J. Am. Chem. Soc.* **1996**, *118*, 267−268.
(11) Mecking, S.; Johnson, L. K.; Wang, L.; Brookhart, M. *J. Am. Chem. Soc.* **1998**, *120*, 888−899.
(12) Ittel, S. D.; Johnson, L. K.; Brookhart, M. *Chem. Rev.* **2000**, *100*, 1169−1204.
(13) Drent, E.; Dijk, R. v.; Ginkel, R. v.; Oort, B. v.; Pugh, R. I. *Chem. Commun.* **2002**, 744−745.
(14) Guironnet, D.; Roesle, P.; Rünzi, T.; Göttker-Schnetmann, I.; Mecking, S. *J. Am. Chem. Soc.* **2009**, *131*, 422−423.
(15) Piche, L.; Daigle, J.-C.; Rehse, G.; Claverie, J. P. *Chem.-Eur. J.* **2012**, *18*, 3277−3285.
(16) Guironnet, D.; Caporaso, L.; Neuwald, B.; Göttker-Schnetmann, I.; Cavallo, L.; Mecking, S. *J. Am. Chem. Soc.* **2010**, *132*, 4418−4426.
(17) Corradini, P.; Guerra, G.; Cavallo, L. *Acc. Chem. Res.* **2004**, *37*, 231−241.
(18) Tshuva, E. Y.; Goldberg, I.; Kol, M. *J. Am. Chem. Soc.* **2000**, *122*, 10706−10707.
(19) Mitani, M.; Saito, J.; Ishii, S.-I.; Nakayama, Y.; Makio, H.; Matsukawa, N.; Matsui, S.; Mohri, J.-i.; Furuyama, R.; Terao, H.; Bando, H.; Tanaka, H.; Fujita, T. *Chem. Rec.* **2004**, *4*, 137−158.
(20) Makio, H.; Terao, H.; Iwashita, A.; Fujita, T. *Chem. Rev.* **2011**, *111*, 2363−2449.
(21) Brookhart, M.; Wagner, M. I.; Balavoine, G. G. A.; Haddou, H. A. *J. Am. Chem. Soc.* **1994**, *116*, 3641−3642.
(22) Aeby, A.; Consiglio, G. *Inorg. Chim. Acta* **1999**, *296*, 45−51.
(23) Bianchini, C.; Meli, A. *Coord. Chem. Rev.* **2002**, *225*, 35−66.
(24) Nozaki, K.; Sato, N.; Tonomura, Y.; Yasutomi, M.; Takaya, H.; Hiyama, T.; Matsubara, T.; Koga, N. *J. Am. Chem. Soc.* **1997**, *119*, 12779−12795.
(25) Sesto, B.; Consiglio, G. *Chem. Commun.* **2000**, 1011−1012.
(26) Sesto, B.; Consiglio, G. *J. Am. Chem. Soc.* **2001**, *123*, 4097−4098.
(27) Noda, S.; Nakamura, A.; Kochi, T.; Chung, L. W.; Morokuma, K.; Nozaki, K. *J. Am. Chem. Soc.* **2009**, *131*, 14088−14100.

(28) Nozaki, K.; Kusumoto, S.; Noda, S.; Kochi, T.; Chung, L. W.; Morokuma, K. *J. Am. Chem. Soc.* **2010**, *132*, 16030−16042.
(29) This consideration also applies to recently reported phosphine-phosphineoxide coordinated catalysts: Carrow, B. P.; Nozaki, K. *J. Am. Chem. Soc.* **2012**, *134*, 8802−8805.
(30) Skupov, K. M.; Marella, P. R.; Simard, M.; Yap, G. P. A.; Allen, N.; Conner, D.; Goodall, B. L.; Claverie, J. P. *Macromol. Rapid Commun.* **2007**, *28*, 2033−2038.
(31) Liu, S.; Borkar, S.; Newsham, D.; Yennawar, H.; Sen, A. *Organometallics* **2007**, *26*, 210−216.
(32) Vela, J.; Lief, G. R.; Shen, Z.; Jordan, R. F. *Organometallics* **2007**, *26*, 6624−6635.
(33) Anselment, T. M. J.; Wichmann, C.; Anderson, C. E.; Herdtweck, E.; Rieger, B. *Organometallics* **2011**, *30*, 6602−6611.
(34) Piche, L.; Daigle, J.-C.; Poli, R.; Claverie, J. P. *Eur. J. Inorg. Chem.* **2010**, 4595−4601.
(35) Kochi, T.; Yoshimura, K.; Nozaki, K. *Dalton Trans.* **2006**, 25−27.
(36) Kochi, T.; Nakamura, A.; Ida, H.; Nozaki, K. *J. Am. Chem. Soc.* **2007**, *129*, 7770−7771.
(37) Anselment, T. M. J.; Anderson, C. E.; Rieger, B.; Boeddinghaus, M. B.; Fassler, T. F. *Dalton Trans.* **2011**, *40*, 8304−8313.
(38) Kochi, T.; Noda, S.; Yoshimura, K.; Nozaki, K. *J. Am. Chem. Soc.* **2007**, *129*, 8948−8949.
(39) (a) Nakamura, A.; Munakata, K.; Kochi, T.; Nozaki, K. *J. Am. Chem. Soc.* **2008**, *130*, 8128−8129. (b) Conley, M. P.; Jordan, R. F. *Angew. Chem., Int. Ed.* **2011**, *50*, 3744−3746. (c) Newsham, D. K.; Borkar, S.; Sen, A.; Conner, D. M.; Goodall, B. L. *Organometallics* **2007**, *26*, 3636−3638.
(40) Wucher, P.; Caporaso, L.; Roesle, P.; Ragone, F.; Cavallo, L.; Mecking, S.; Göttker-Schnetmann, I. *Proc. Natl. Acad. Sci. U.S.A.* **2011**, *108*, 8955−8959.
(41) (a) Hearley, A. K.; Nowack, R. J.; Rieger, B. *Organometallics* **2005**, *24*, 2755−2763. (b) Rünzi, T.; Guironnet, D.; Göttker-Schnetmann, I.; Mecking, S. *J. Am. Chem. Soc.* **2010**, *132*, 16623−16630. (c) Friedberger, T.; Wucher, P.; Mecking, S. *J. Am. Chem. Soc.* **2012**, *134*, 1010−1018. (d) Ito, S.; Munakata, K.; Nakamura, A.; Nozaki, K. *J. Am. Chem. Soc.* **2009**, *131*, 14606−14607.
(42) Note that for bulky nonchelating aryl moieties, for example, C_6H_4Et, $C_6H_4(2,6\text{-}(OMe)_2C_6H_3)$, and 1-methoxynaphatalene, a distortion of the chelate ring toward a half-boat conformation with the palladium, or the oxygen bound to the palladium, placed at the top position is observed.[30,32,33]
(43) Neuwald, B.; Ölscher, F.; Göttker-Schnetmann, I.; Mecking, S. *Organometallics* **2012**, *31*, 3128−3137.
(44) Mislow, K. *Acc. Chem. Res.* **1976**, *9*, 26−33.
(45) The mechanism of transformation is discussed in the Supporting Information.
(46) Differences are found for coalescence temperature and the adopted exo configuration. The free ligands ^{MeO}**(P^O)H**, ^{CF3}**(P^O)H**, ^{Ar}**(P^O)H** and their salts adopt an exo_3 configuration in solution, whereas the complexes ^{MeO}**1**, ^{CF3}**1** adopt an exo_2 configuration in line with the solid-state structures.
(47) In addition, DFT calculations for ^{MeO}**1**, $^{(MeO)2}$**1**, ^{Ar}**1**, and $^{Ar/(MeO)2}$**1** are in line with the experimental results. Energy barriers for the ring flip transition state were found to be always below 30 kJ/mol, whereas barriers for the aryl rotation process are at least 10 kJ/mol higher in energy and range from 36 to 63 kJ/mol (cf., Supporting Information Table S24).
(48) Friebolin, H. *Basic One- and Two-Dimensional NMR Spectroscopy*, 4th ed.; Wiley-VCH: Weinheim, Germany, 2005.
(49) Note that as a whole group CF_3 is much smaller than 2,6-$(MeO)_2C_6H_3$, but that for the steric interaction the steric bulk directly attached at the P-aryls appears decisive, which leads to a similar influence on the rotational barrier for the tetrahedral CF_3- versus the flat aryl-substituent.
(50) However, for the protonated ligand $^{Ar/(MeO)2}$**(P^O)H**, no formation of diastereomers can be observed down to −90 °C ($\Delta G^{\ddagger}_{Tc\text{-}Ar/(MeO)2(P^O)H}$ < 35 kJ/mol), but a rather high barrier of 52 kJ/mol is found for an isolated process only affecting the rotation of the $(MeO)_2C_6H_3$ aryl substituent at the phosphorus atom (cf., Supporting Information).
(51) The rac/meso designation is based on consideration of the stereocenters as part of a growing chain. The two stereocenters can possess identical (^{MeO}**3**$_{MA\text{-}meso}$) or opposite (^{MeO}**3**$_{MA\text{-}rac}$) stereoconfiguration. The absolute assignment is based on a reinvestigation of the corresponding X-ray structure (ref 16) and is in line with NOESY/ROESY experiments in solution. Note that within experimental error the ratios of the integrals of different resonances in Figure 7 are all identical, and agree with a slight preference for the rac isomer (ca. 2:1).
(52) Ziegler, T.; Autschbach, J. *Chem. Rev.* **2005**, *105*, 2695−2722.
(53) Haras, A.; Anderson, G. D. W.; Michalak, A.; Rieger, B.; Ziegler, T. *Organometallics* **2006**, *25*, 4491−4497.
(54) Differences between the ring flip and aryl rotation barriers for the olefin complexes are nearly identical to the corresponding monomer-free complexes ^{X}**1** (cf., Supporting Information).
(55) For all systems, the TS for the consecutive 1,2−1,2 MA insertion is at least 25 k/J mol higher than for the corresponding consecutive 2,1−2,1 MA insertion TS.
(56) Nakamura, A.; Kageyama, T.; Goto, H.; Carrow, B. P.; Ito, S.; Nozaki, K. *J. Am. Chem. Soc.* **2012**, *134*, 12366−12369.